LAWRENCE
LIVERMORE
NATIONAL
LABORATORY

LLNL-CONF-415032

An atomic inner-shell laser pumped with an x-ray free-electron laser

N. Rohringer

July 24, 2009

ICPEAC -International conference on photonic, electronic, and atomic collisions
Kalamazoo, MI, United States
July 22, 2009 through July 28, 2009

Disclaimer

An Atomic Inner-Shell Laser Pumped with an X-Ray Free-Electron Laser

Nina Rohringer

Lawrence Livermore National Laboratory, 7000 East Avenue, Livermore, California 94551, USA

E-mail: rohringer1@llnl.gov

Abstract. Focusing an x-ray free electron laser (XFEL) pulse into a gas target, a plasma of transiently core excited ions can be created within a few femtoseconds, building a pathway to an inner-shell keV atomic x-ray laser. Varying the XFEL parameters, a wide variety of pulse structures can be created with comparable peak-intensities to XFELs: isolated pulses of sub-femtosecond duration, trains of pulses with increased temporal coherence, and trains of femtosecond pulses of different wavelengths. We present self-consistent gain and amplification calculations, tailored to predict first experiments on lasing on neon pumped by the Linac Coherent Light Source at Stanford.

1. Introduction

Recently, lasing of the first x-ray free electron laser (XFEL) – the Linac Coherent Light Source [1] (LCLS) at Stanford – was demonstrated at 8 keV photon energy [2]. Worldwide, other two XFEL facilities are currently under construction [3, 4]. These x-ray sources will be based on the self-amplified spontaneous emission (SASE) process [5, 6, 7]. This process creates pulses of chaotic temporal and spectral intensity profile. The created pulses can be seen as an ensemble of phase uncorrelated intensity spikes of femtosecond (fs) duration, of random width, height, position and phase. In case of LCLS, pulses will have a $30-100$ fs duration with coherence a time of 2-3 fs at 1 keV photon energy. The unprecedented high peak brilliance of SASE XFELs will open the pathway to study non-linear optical processes in the x-ray regime for the first time [8]. These processes depend on higher order coherence properties of the XFEL, which makes the interpretation of experimental results and determining fundamental cross-sections for non-linear optical processes a delicate, difficult task [9, 10, 11, 12, 13, 14, 15]. Fundamental quantum optical processes in the x-ray regime, as an example Rabi-flopping involving a core electron [16], require isolated pulses of fs duration, in order to be observed in the time domain. Hence, a control of the pulse duration and isolating single x-ray pulses of fs duration would be an advantage for applications in quantum optics and for interpreting the results of multi-photon processes in the x-ray regime. In this contribution we give a theoretical case study, exploring the possibility to pump an inner-shell atomic x-ray laser with an XFEL. This will open the pathway to a wide variety of x-ray pulse structures with peak intensities comparable to those of the pumping XFEL and wavelengths of 1.5 nm or less. We show that it might become possible to isolate single pulses of sub-fs duration, to create a train of pulses of improved temporal coherence and to produce a series of temporally separated fs pulses of different wavelengths, suitable for applications in

multi-color x-ray pump-probe experiments.

The challenge of producing ultrashort high-intensity x-ray sources is being tackled by several techniques. Recently, a proposal was put forward to produce a train of attosecond pulses by mode locking of an XFEL [17]. Other XFEL-based techniques are based on slicing of the electron beam [18] or operation with low-charge, ultra-low emittance electron beams [19]. A completely different approach is an optical laser pumped XRL seeded with high-harmonic radiation [20]. Due to the lack of high-harmonic radiation at shorter wavelength, this method is currently limited to the soft x-ray regime ($>$ 10 nm). Recently, the idea of using an FEL to pump a laser in the XUV regime was put forward for an inner-shell lasing scheme of carbon [21] and a recombination-based soft XRL of helium [22]. We propose a lasing scheme of broad capability, by photo-pumping an inner-shell XRL [23] with an XFEL. The method can be applied to a broad variety of gain materials. In this contribution we present gain calculations for neon, to simulate first lasing experiments using the LCLS.

The article is organized as follows: in the next section we describe the lasing scheme. In section 3 we discuss results of small-signal gain calculations at different photon pumping energies. In section 4, we present the one-dimensional self-consistent gain model to determine the X-ray laser output and show results for pumping with 1 keV and 1.4 keV photon energy.

2. Description of the inner-shell lasing scheme

We propose to use an XFEL to create a population inversion by inner-shell photoionization. The concept of a photoionization-pumped x-ray laser dates back more than fourty years [23, 24], but due to the lack of appropriate x-ray pumping sources, it could not be experimentally realized so far. XFELs are opening doors into unprecedented territory. Focusing an XFEL into a gas target, an elongated plasma column of core-excited ions is created by inner-shell photoionization within the first few fs of the XFEL pulse [15]. The core-excited ions relax by either Auger decay or radiative decay. In case of neon, the Auger lifetime of a K-shell hole is 2.7 fs, therefore allowing a transient population inversion of only fs duration. This short lived population inversion forms the basis of ultra-short the x-ray transition. Since the build-up of population inversion happens on an ultrafast time scale (typically during the first few intensity spikes of the SASE pump), i.e. fast compared to typical ion-electron collision times in a gas target of moderate density, the ion temperature in the plasma column is expected to remain cold.[1] The line width of the lasing transition is then dominated by the Auger width of the core-hole, which opens the pathway to very narrow, high-gain lasing transitions. This is in strong contrast to traditional optical-laser pumped atomic XRLs [25, 26], where the line width is dominated by Doppler and Stark broadening for hot, high density plasmas.Our proposed lasing scheme is self-terminating, i.e. each atom can at most contribute one photon of a given transition during the amplification process. The lower lasing state in our pumping scheme is efficiently depleted by another inner-shell photoionization event. This is in contrast to recently proposed XUV FEL pumped lasing schemes between two auto-ionizing states [21], where depletion of the lower lasing level is caused by Coster-Kronig transitions. Our scheme is widely applicable, by tuning the pumping photon energy above the core-ionization edge of the lower lying lasing state and can be extended to any other atomic species.

The geometry of the XRL is determined by the focus of the XFEL. Focusing an XFEL pulse of 1 keV photon energy with a supposed Gaussian spatial beam profile to a focal radius of $r = 1$ μm results in a focal depth of approximately 5 mm, which defines the length L of the amplifying plasma column. The transverse coherence length of the XRL can be characterized

[1] We estimated the electron-ion collision time τ by a simple geometrical approach [24]. Pumping neon with 1 keV photon energy will produce slow photoelectrons of $\sim$ 100 eV energy and hot Auger electrons with energies of $\sim$ 800 eV. Supposing a gas density of 10^{19} cm^{-3}, the electron-ion collision time for the photoelectrons will be around $\tau \sim 800$ fs, that for Auger electrons $\tau \sim 570$ fs, i.e. long compared to the XFEL pulse duration.

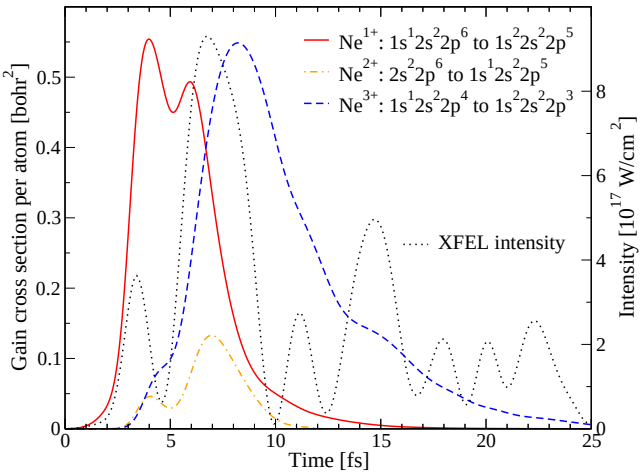

Figure 1. Small-signal gain cross section per atom for the strongest transitions in singly, doubly and triply ionized neon for a sample XFEL pulse of 1 keV photon energy. For the XFEL pulse we assumed 5×10^{12} photons, a pulse duration of 100 fs and a focus spot diameter of 2μm.

by the geometry of the amplifying plasma column [27] and is given by $L_T = \frac{\lambda L}{2\pi r}$. For a lasing transition around $\lambda = 1$ nm, we therefore find a transverse coherence length of $L_T = 1$ μm, implying that the XRL will basically have full spatial coherence and a single transverse mode.

3. Small signal gain calculations

Amplification of spontaneous emission in the exponential gain regime is determined by the small signal gain cross section. The small-signal gain cross section per atom is defined as

$$g(t) = n_U(t)\sigma_{stim} - n_L(t)\sigma_{abs} \ , \tag{1}$$

where n_U and n_L are the occupancies of the upper and lower lasing states. σ_{stim} and σ_{abs} are the cross-sections for stimulated emission and absorption, given by

$$\sigma_{stim} = A_{U\to L}\frac{2\pi c^2}{\omega^2 \Delta\omega} \ , \quad \sigma_{abs} = \sigma_{stim}\frac{g_U}{g_L} \ , \tag{2}$$

where $A_{U\to L}$ is the Einstein A coefficient for the radiative transition and g_U and g_L are the statistical weights of the upper and lower lasing levels. Eq. (2) gives the cross sections at the peak of the line, supposing a Lorentzian line shape. The line width $\Delta\omega$ is dominated by the total lifetime of the upper and lower states. The relative natural line widths of the dominant x-ray lasing transitions in neon are listed in Table 1 and are typically $10^{-5} - 10^{-4}$ for Auger-decay broadened lines and $\sim 5 \times 10^{-6}$ in the case of the hydrogen-like Ne^{9+} 2p-1s transition. Hence, extremelly narrow line width can be achieved with the proposed scheme.

The occupancies n_U and n_L to determine the small signal gain-cross section of Eq. (1) are determined by the influence of the XFEL pump radiation on an ensemble of single atoms by solving a system of rate equations, describing valence and core photoionization, Auger decay and radiative decay [15]. In total, we treat 63 different configurations states, up to Ne^{10+} and simulate the chaotic intensity profile of the SASE XFEL radiation with a Monte Carlo method [28].

Figure 1 shows the temporal evolution of the small-signal gain cross sections of singly, doubly and triply ionized neon for a typical XFEL SASE pulse at 1 keV photon energy. The gain maxima are temporally correlated with the maxima of the intensity spikes of the XFEL pump and are separated by a few fs. The first two XFEL spike ionize an K-shell electron, creating a population inversion between the the levels 1s^{1}2s^{2}2p^6 and 1s^{2}2s^{2}2p^5 of Ne^{1+}. The width of the Ne^{1+} transition line is determined by the Auger lifetime of the core hole, which is 2.75 fs.

Table 1. Saturation intensity, average of the peak value and the duration (FWHM) of the dominant small-signal gains and their standard deviation for an ensemble of 10,000 random pulses for $\omega_P = 1.4$ keV. For the XFEL pump pulse, we supposed an average number of 5×10^{12} photons, 100 fs duration and a focal diamter of 2 μm.

Ne	upper state	ω [eV]	$\Delta\omega/\omega$	gain [a.u.]	$\mathrm{STD}_{\mathrm{gain}}$	τ[fs]	STD_τ	I_{sat}[W/cm^2]
1+	$1s^1 2s^2 2p^6$	849.8	2.9×10^{-4}	0.466	0.101	5.3	2.4	9.3×10^{14}
3+	$1s^1 2s^2 2p^4$	861.9	2.1×10^{-4}	0.199	0.041	7.2	3.2	6.6×10^{14}
5+	$1s^1 2s^1 2p^3$	879.9	1.1×10^{-4}	0.126	0.040	4.4	2.3	2.0×10^{14}
5+	$1s^1 2s^2 2p^2$	880.4	1.2×10^{-4}	0.092	0.015	10.9	4.9	3.5×10^{14}
7+	$1s^1 2p^2$	902.6	3.2×10^{-5}	0.351	0.090	5.9	4.2	2.6×10^{13}
7+	$1s^1 2s^1 2p^1$	903.7	1.6×10^{-5}	0.506	0.042	26.3	7.6	1.2×10^{13}
8+	$1s^1 2p^1$	916.4	1.5×10^{-6}	0.364	0.198	39.8	28.1	1.1×10^{11}
8+	$2p^2$	1006.9	7.9×10^{-5}	0.698	0.234	12.7	12.4	8.3×10^{13}
8+	$2s^1 2p^1$	1008.6	3.5×10^{-5}	0.896	0.127	40.6	24.3	3.6×10^{13}
9+	$2p^1$	1022.0	4.0×10^{-6}	6.131	2.718	14.9	12.2	4.4×10^{11}

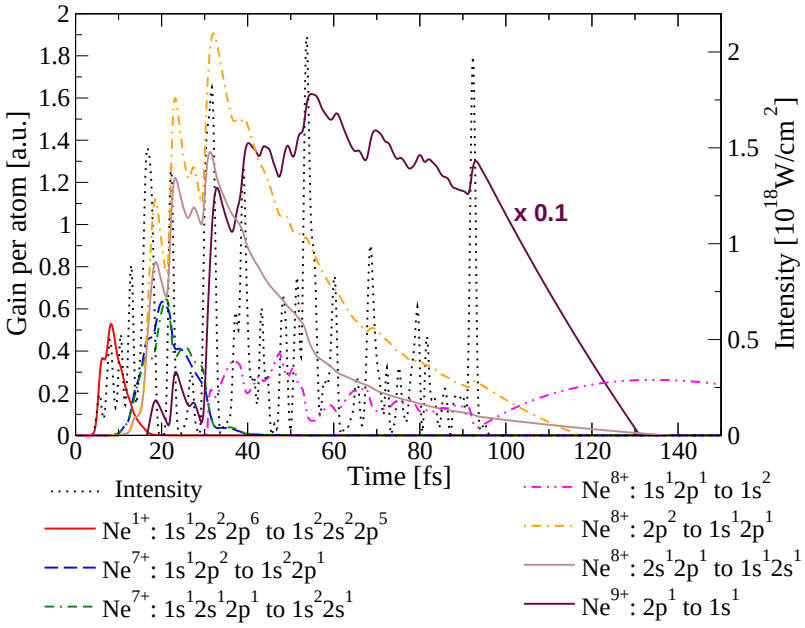

Figure 2. Dominant small signal gain cross sections g and the XFEL intensity as a function of time. We supposed a XFEL pump pulse of 100 fs duration containing 5×10^{12} photons of 1.4 keV energy and a focus diameter of 1.2 μm. At a density of $n = 10^{18}$ cm^{-3} the gain coefficient $G = gn$ (in mm^{-1}) is related to the gain cross section (in bohr^2) by $G = 2.8g$. Typically, the XRL saturates at a gain-length product $GL \sim 20$ [26]. Hence, saturation can be achieved with an interaction length of a few mm.

The probability to produce a double core-hole in the K-shell by another photoionization event, before Auger decay of the 1s hole takes place, is small – hence a small cross-section of the Ne^{2+} $2s^2 2p^6$ to $1s^1 2s^2 2p^5$ transition. The dominant Auger decay channel of the core-excited Ne^{1+} is to Ne^{2+} $2s^2 2s^2 2p^4$. This state is subsequently core ionized by the XFEL pulse, giving rise to the second strongest transition from Ne^{3+} $1s^1 2s^2 2p^4$. For the particular sample pulse chosen, the peak gain-cross sections for the Ne^{1+} and Ne^{3+} transition are of similar size. This implies, that it is possible to saturate both lasing transitions. This observation will be corrobated by a one-dimensional self-consistent gain calculation, which will be presented in the next section.

Pumping with 1.4 keV photon energy, core-excited, long lived helium and hydrogen-like states in neon become accessible (see Figure 2, showing the small-signal gain cross sections). Transitions resulting from these states have extremely narrow natural widths in the order of

$10^{-6} - 10^{-5}$. This opens the pathway to a XRL source of increased longitudinal (temporal) coherence length L_L, which can be estimated by $L_L = \lambda^2/\Delta\lambda$. In case of the hydrogen-like transition in neon at $\lambda = 1.2$ nm this would result in a coherence length $L_L = 300$ μm, or a longitudinal coherence time of approximately one picosecond, i.e. the pulses created would have full temporal coherence. This would be a great improvement to SASE FEL pulses.

Due to the chaotic nature of the XFEL pump, small-signal gain cross sections and hence the output of the XRL will vary on a shot-to-shot basis. We therefore averaged the cross sections over an ensemble of random pulses. The general trend of the averaged temporal gain-profiles is similar to that of the single-shot profiles. The average values and standard deviations of the peak gain cross section, as well as their duration at FWHM and saturation intensity is given in Table 1 for 1.4 keV photon energy.

4. Self-consistent gain calculations

In previous work [29] we have studied lasing from a single lasing transition corresponding to the highest small-signal gain cross section. In this contribution, we extended our self-consistent gain model to several lasing states, in order to study, if saturation of more than one lasing transition becomes possible, as inferred from the small-signal gain calculations. To simulate the output of the lasing transitions, we apply a one-dimensional model that couples the atomic level kinetics to the laser propagation and amplification. Due to the longitudinal pumping, lasing occurs only in forward direction. This was verified numerically. In our model, we treat valence and core ionization by the XFEL pump radiation, spontaneous and stimulated radiative decay and Auger decay. The rate equation for determining the occupation of the upper and lower lasing states N_U^M and N_L^M at position z and time t, where M denotes the ionic charge state, U and L is an index defining the atomic configuration of the upper and lower lasing states, are determined by:

$$\begin{aligned}
\frac{dN_U^M(z,t)}{dt} &= \sum_i \sigma_i^v j(z,t) N_i^{M-1}(z,t) + \sum_i \sigma_i^c j(z,t) N_i^{M-1}(z,t) \\
&\quad - \left[A_{k\to l} + p_U^A + (\sigma_U^v + \sigma_U^c) j(z,t)\right] N_U^M(z,t) \\
&\quad - \sigma^{se} j_U^{XRL}(z,t) N_U^M(z,t) + \sigma^{abs} j_U^{XRL}(z,t) N_L^M(z,t) \qquad (3) \\
\frac{dN_L^M(z,t)}{dt} &= \sum_i \sigma_i^v j(z,t) N_i^{M-1}(z,t) + \sum_i \sigma_i^c j(z,t) N_i^{M-1}(z,t) - \left[\sigma_L^v - \sigma_L^c\right] j(z,t) N_L^M(z,t) \\
&\quad + \sigma^{se} j_U^{XRL}(z,t) N_U^M(z,t) - \sigma^{abs} j_U^{XRL}(z,t) N_L^M(z,t)\,, \qquad (4)
\end{aligned}$$

where σ_i^v and σ_i^c denote the cross section for valence and core photoionization [30] respectively for a general state i (not necessary a state giving rise to a lasing transition) with occupation N_i^{M-1}. The propagating flux of the XFEL pump pulse is denoted by $j(z,t)$ and p_U^A is the total Auger decay rate of the upper lasing state. Absorption of the XFEL pump $j(z,t)$ is taken into consideration, by an additional differential equation coupled to Eqs. (3) and (4). Ampflification and propagation of the XRL flux j_U^{XRL} from transition $U \to L$ is determined by

$$\frac{dj_U^{XRL}}{dt} = j_U^{XRL}(z,t) c n_A \left[\sigma^{se} N_U^M(z,t) - \sigma^{abs} N_L^M(z,t)\right] + \frac{\Omega(z)}{4\pi} A_{U\to L} N_U^M(z,t) n_A c - c\frac{dj_U^{XRL}}{dz}\,, \quad (5)$$

where $z \in [0, L]$, $\Omega(z) = 2\pi[1 - (L-z)/\sqrt{r^2 + (L-z)^2}]$ is the solid geometrical acceptance angle, allowing propagation in forward direction, n_A is the atomic density, L the interaction length, and r the focal radius.

Fig. 3 shows the results of the self-consistent gain calculations for the sample pulse of Figure 1. Shown are the peak intensities (a) and the peak gain cross sections (b) for the dominant lasing transitions of singly, doubly and triply ionized neon as a function of the interaction length, for

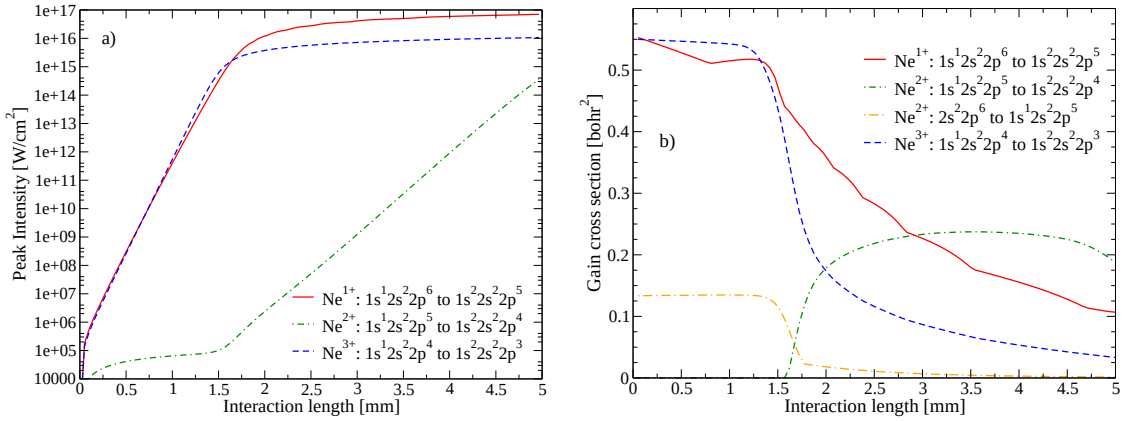

Figure 3. Peak intensities (a) and Peak gain cross sections (b) of the dominant XRL transitions of singly, doubly and triply ionized neon as a function of the interaction length, as determined from the level occupancies resulting from the self-consistent gain model. Parameters of the XFEL pulse are given in Figure 1. We assumed an atomic density of 10^{19} atoms/cm^3.

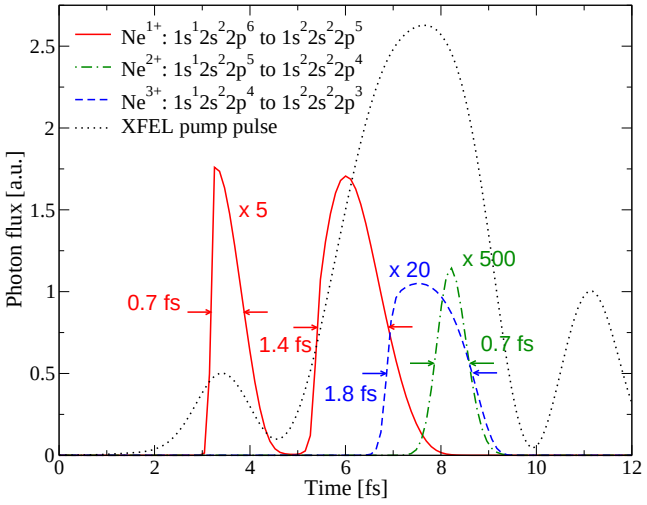

Figure 4. Output flux in a.u. of the dominant XRL lines and the transmitted XFEL pump pulse (at 1 keV photon energy) as a function of time. For better visibility, the XRL fluxes have been scaled.

a photon pump energy of 1 keV. The Ne^{1+} 1s^{1}2s^{2}2p^6 to 1s^{2}2s^{2}2p^5 transition (850 eV) and Ne^{3+} 1s^{1}2s^{2}2p^4 to 1s^{2}2s^{2}2p^3 (862 eV) have similar initial small-signal gain (see Fig. 1). Both lines amplify exponentially with approximately the same gain and start to saturate at $\sim$ 1.5 mm. At the exit of the plasma column there are $\sim 3 \times 10^{10}$ photons in the Ne^{1+} transition, $\sim 4 \times 10^9$ photons in the Ne^{3+} transition. Once saturation sets in, the level occupancies change dramatically, i.e. the stimulated emission becomes faster than the Auger-decay. In this regime, the amplification is no longer determined by the small-signal gain cross sections. Transition lines, which initially had no positive gain cross section, suddenly show finite gain and amplify exponentially. As soon as the Ne^{1+} transition saturates, Ne^{1+} 1s^{2}2s^{2}2p^5 is efficiently populated by stimulated emission. This state is subsequently core-ionized. As a consequence, the gain cross-section of the Ne^{2+} 1s^{1}2s^{2}2p^5 to 1s^{2}2s^{2}2p^4 transition (855 eV) kicks up, whereas the gain of the initially dominant transition of the double-core excited Ne^{2+} 2s^{2}2p^6 drops. The slight non-monotonic, bumpy structure of the gain cross section of the Ne^{1+} transition as a function of z is caused by the temporal double-hump structure of the initial gain and the absorption of the XFEL pump radiation.

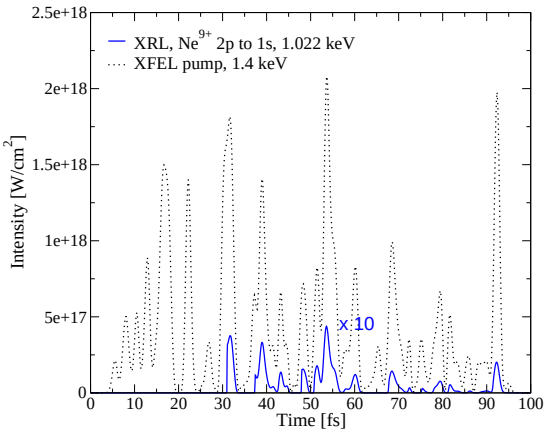

Figure 5. Output intensity of the hydrogen like XRL line (Ne^{9+} 2p to 1s at 1.022 keV) and the XFEL pump pulse (at 1.4keV photon energy) as a function of time at the exit of the amplifying plasma column for a gas density of 10^{18}cm^{-3}. The XRL intensity has been scaled by a factor of 10. The XFEL pulse of 100 fs duration was assumed to be focused to a a diameter of 1.2 μm and contains 5×10^{12} photons. The number of photons in the emitted XRL pulse train is 7×10^9.

The temporal output profile of the different XRL lasing lines is shown in Fig. 4, showing the flux as a function of time for the XRL lines and the transmitted XFEL pulse. For the particular XFEL sample pulse, the Ne^{1+} transition (at 850 eV) results in two pulses of 0.7 fs and 1.4 fs pulse duration (FWHM), separated by 3 fs. The Ne^{3+} transition (at 862 eV) has a pulse duration of 1.8 fs and has a flux that is a factor of 4 smaller than that of the Ne^{1+} transition. We want to emphasize that these results are for a particular sample shot. Pulse duration, the number of pulses (typically 1-2) at a given wavelength and their relative peak intensities will vary on a shot-to-shot basis. It is therefore possible, that for a subset of XFEL pulses, the Ne^{3+} lasing line cannot be saturated. The reason for this is that once the Ne^{1+} saturates, also the gain of the Ne^{3+} transitions drops, due to the change in level kinetics. In cases, where the initial small-signal gain of Ne^{3+} was considerable smaller than that of Ne^{1+}, the amplification of Ne^{3+} is hence quenched as soon as saturation of Ne^{1+} sets in, and the Ne^{3+} will not reach saturation. The lasing transition resulting from the Ne^{2+} $1s^1 2s^2 2p^5$ state has a duration of 0.7 fs. Although its peak intensity is a factor of 100 smaller than that of the Ne^{1+} line, there are still $\sim 6 \times 10^7$ photons contained in this pulse. This total number of photons is comparable to sub-fs VUV sources composed of higher-harmonic radiation of optical laser pulses and hence can serve as a probe pulse in a multi-color x-ray pump-probe application of our proposed XRL.
The expected XRL output for pumping with 1.4 keV photon energy is shown in Figure 5, where the temporal profile of the hydrogen-like 2p-1s transition of Ne^{9+} is shown. The XRL output consists of a train of pulses of fs duration, streching over a time span of 70 fs. The intensity profile follows the spike profile of the pumping SASE pulse, but in contrast to the SASE radiation, the spikes created in the XRL will have a fixed phase relation and the pulse has full temporal coherence, albeit at lower peak intensities.

5. Conclusions

In this paper we presented detailed self-consistent gain calculations of a recently proposed inner-shell atomic XRL pumping scheme [29] using SASE XFEL radiation. We discussed results on neon in a parameter regime which corresponds to planned experiments at the LCLS. As inferred from the small-signal gain cross sections for neon, it is possible to subsequently saturate more than one lasing transition, pertaining to different ionic charge states, i.e. producing a series of fs x-ray pulses of different wavelengths, at intensities comparable to that of the pumping XFEL. The pulse structures, durations and intensities will vary, however, on a shot-to-shot basis, due to the chaotic nature of the SASE XFEL pump pulse. Pumping with 1.4 keV photon energy, lasing of the hydrogen-like 2p-1s transition can be exploited, transforming SASE FEL pulses into a train of mutually phase coherent fs pulses. The proposed inner-shell ionization XRL pumping scheme could open pathways towards high-intensity x-ray radiation of increased

temporal coherence and multi-color non-linear pump-probe experiments in the x-ray regime.

Acknowledgments
Work supported by the U.S. Department of Energy under contract No. DE-AC52-07NA27344; support from the Laboratory Directed Research and Development Program at LLNL is also acknowledged.

References

[1] Arthur *et al* J 2002 *Linac Coherent Light Source (LCLS) Conceptual Design Report* (Stanford Linear Accelerator Center, SLAC report 593)
[2] Emma P for the LCLS commissioning team *Proc. of the 2009 Part. Acc. Conf., Vancouver, B.C., Canada (IEEE, Piscataway, NJ, 2009)*
[3] Altarelli*et al* M http://xfel.desy.de/tdr/index_eng.html
[4] Tanaka T and Shintake T http://www-xfel.spring8.or.jp/
[5] Pellegrini C and Reiche S 2004 *IEEE J. Sel. Top. Quantum Electron.* **10** 1393
[6] Bonifacio R, Pellegrini C and Narducci L M 2002 *Opt. Commun.* **50** 373
[7] Saldin E L, Schneidmiller E A and Yurkov M V 1998 *Opt. Commun.* **148** 383
[8] Freeman *et al* R R 2000 *LCSL: The first experiments* (Stanford Linear Accelerator Center, SLAC report 611)
[9] Wabnitz H, de Castro A, Gürtler P, Laarmann T, Laasch W, Schulz J and Möller T 2005 *Phys. Rev. Lett.* **94** 023001
[10] Santra R and Greene C 2004 *Phys. Rev. A* **70** 053401
[11] Sorokin A A, Wellhofer M, Bobashev S V, Tiedtke K, and Richter M 2007 *Phys. Rev. A* **75** 051402(R)
[12] Makris M G and Lambropoulos P 2008 *Phys. Rev. A* 023401
[13] Makris M G and Lambropoulos P 2008 *Phys. Rev. A* **77** 023415
[14] Makris M G, Lambropoulos P and Mihelic A 2009 *Phys. Rev. Lett.* **102** 033002
[15] Rohringer N and Santra R 2007 *Phys. Rev. A* **76** 033416
[16] Rohringer N and Santra R 2008 *Phys. Rev. A* **77** 053404
[17] Thompson N R and NcNeil B 2008 *Phys. Rev. Lett.* **100** 203901
[18] Emma *et al* P 2004 *Phys. Rev. Lett.* **92** 074801
[19] Ding *et al* Y 2009 *Phys. Rev. Lett.* **102** 254801
[20] Y Wang *et al* 2008 *Nature photonics* **2** 94
[21] J Zhao *et al* 2008 *Optics Express* **16** 3546
[22] Lan K, Fill E and Meyer-Ter-Vehn J 2004 *Laser Part. Beams* **22** 261
[23] Duguay M A and Rentzepis G P 1967 *Appl. Phys. Lett* **10** 350
[24] Axelrod T S 1976 *Phys. Rev. A* **13** 376
[25] Matthews *et al* D L 1985 *Phys. Rev. Lett.* **54** 110
[26] Elton R C 1990 *X-ray lasers* (Academic Press, Inc.)
[27] London R A 1993 *Phys. Fluids B* **5** 2707
[28] Vannucci G and Teich M C 1980 *Appl. Opt.* **19** 548
[29] Rohringer N and London R 2009 *Phys. Rev. A* **80** 013809
[30] Los Alamos National Laboratory Atomic Physics Codes http://aphysics2.lanl.gov/cgi-bin/ION/runlanl08a.pl